Supporting Information

Superhelices with tunable twisting power directed by supramolecular pairing of focal asymmetry in achiral dendron-jacketed block copolymers

I-Ming Lin,[a] Che-Min Chou,[b] Ming-Chia Li,[c] Rong-Hao Guo,[b] Cheng-Kuang Lee,[d] Han-Jung Li,[d] Yeo-Wan Chiang,[a,g*] Yi-Hung Lin,[b] Yao-Chang Lee,[b] Chun-Jen Su,[b] U-Ser Jeng,[b,e,f] and Wei-Tsung Chuang[b,f*]

[a]Department of Materials and Optoelectronic Science, Center for Nanoscience and Nanotechnology, National Sun Yat-Sen University, Kaohsiung, 80424 (Taiwan)

[b]National Synchrotron Radiation Research Center, Hsinchu, 30076 (Taiwan)

[c]Department of Biological Science and Technology, National Chiao Tung University, Hsinchu, 30010 (Taiwan)

[d]Department of Chemical Engineering, National Tsing Hua University, Hsinchu 30013 (Taiwan)

[e]Material and Chemical Research Laboratories, Industrial Technology Research Institute, Hsinchu, 31040 (Taiwan)

[f.] Graduate Institute of Applied Science and Technology, National Taiwan University of Science and Technology, Taipei, 10607 (Taiwan)

[g.]Department of Fragrance and Cosmetic Science, Kaohsiung Medical University,Kaohsiung, 80708 (Taiwan).

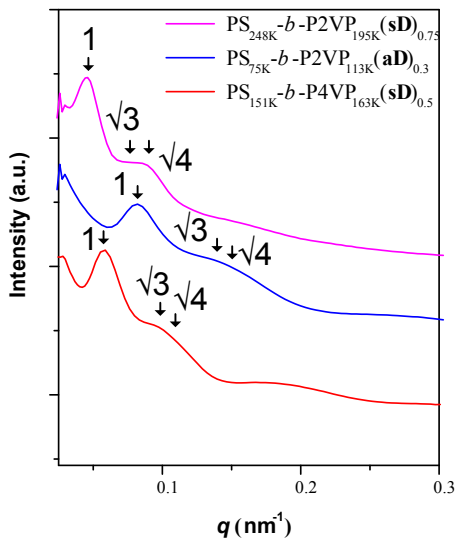

Figure S1. 1D SAXS profiles of DJBCP films. The position ratio 1:√3:√4 indicates the hexagonally packed lattice.

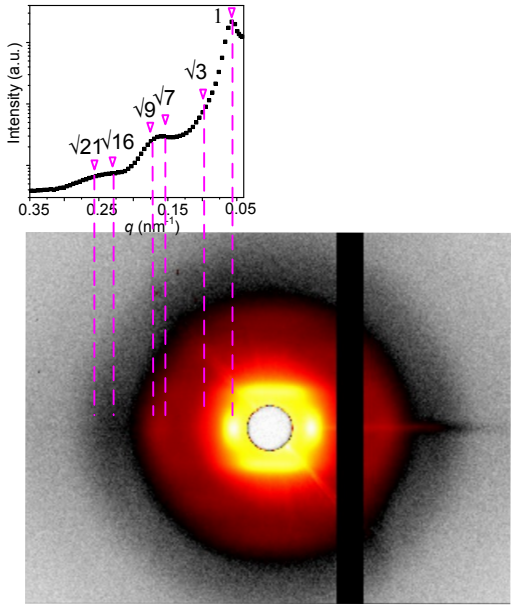

Figure S2. 2D SXAS pattern changed by the color threshold in Fig. 2a for highlight the diffractions along the equatorial direction.

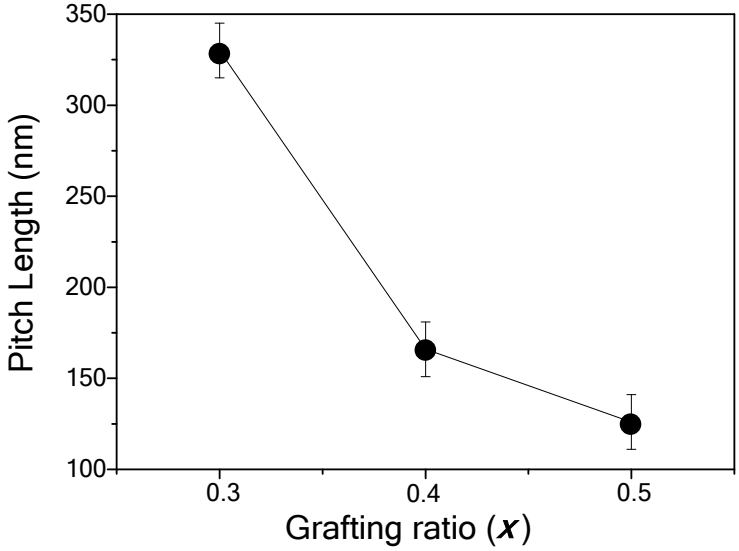

Figure S3. Variation of pitch lengths of PS helices with the grafting ratio for PS_{151K}-*b*-$P4VP_{163K}$(**aD**)$_x$. The data is obtained from both TEM and SAXS results.

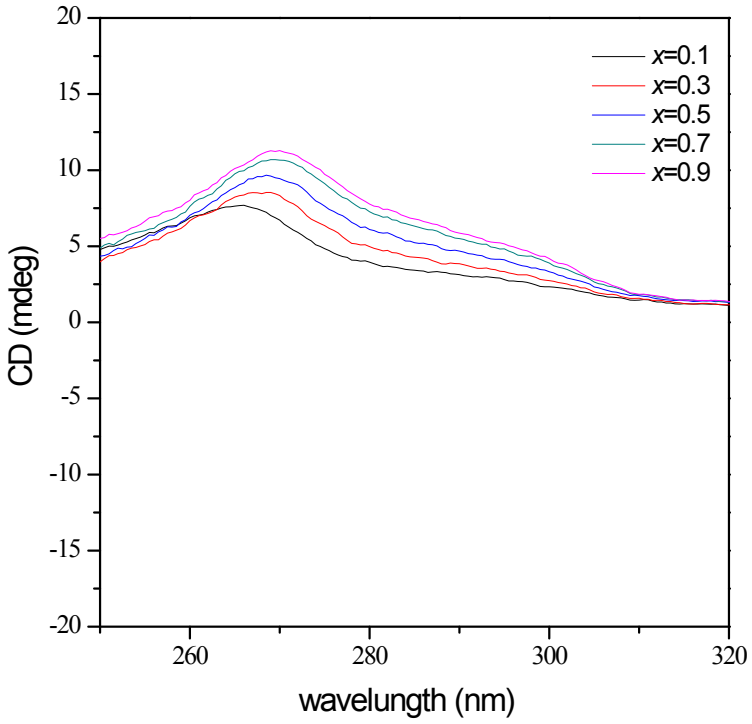

Figure S4. CD spectra of $P4VP_{8.8K}$(**aD**)$_x$ (0.05 mass % in trichloromethane at 25 ^{o}C).

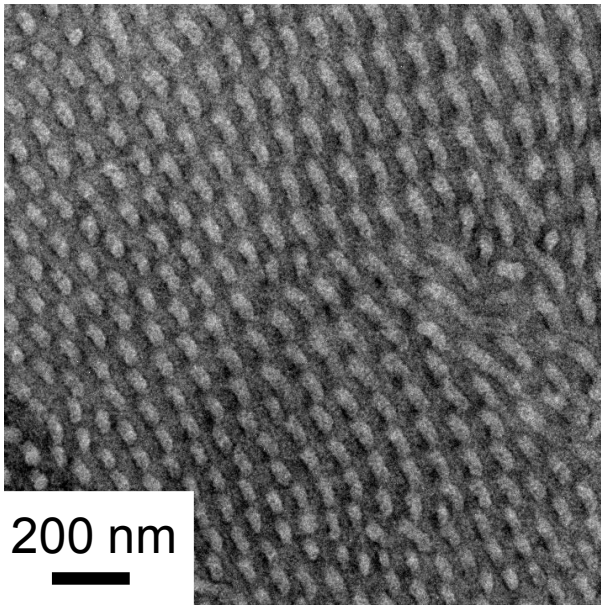

Figure S5. TEM morphology of PS_{75K}-*b*-$P2VP_{113K}$(**sD**)$_{0.3}$.

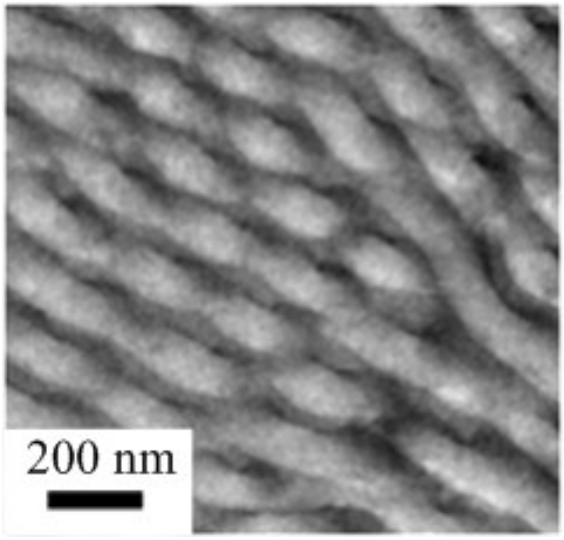

Figure S6. TEM morphology of PS_{248K}-*b*-$P2VP_{195K}$(**PDP**)$_{1.0}$.

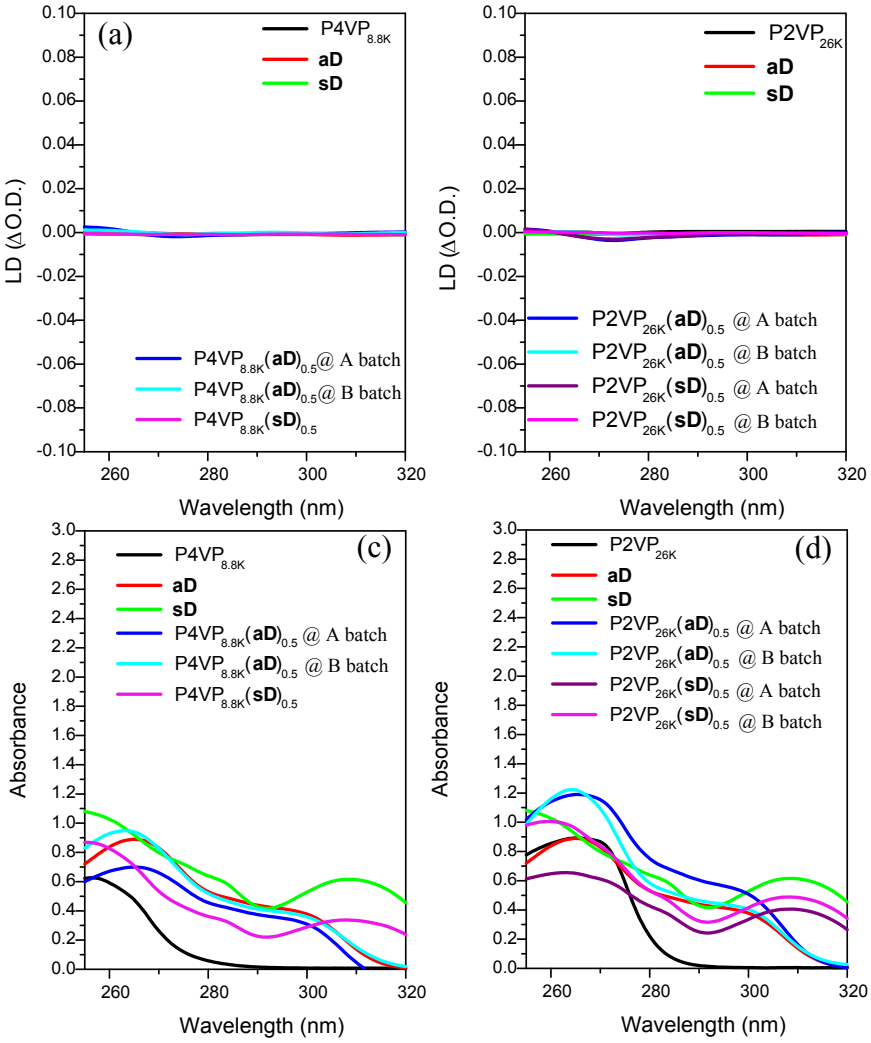

Figure S7. LD spectra of (a) dendron-jacketed P4VP solutions and (b) dendron-jacketed P2VP solutions (0.05 mass % in trichloromethane at 25 °C) and corresponding absorption spectra of (c) dendron-jacketed P4VP solutions and (d) dendron-jacketed P2VP solutions. The neat polymers and dendrons as the control are shown in (a)-(d).

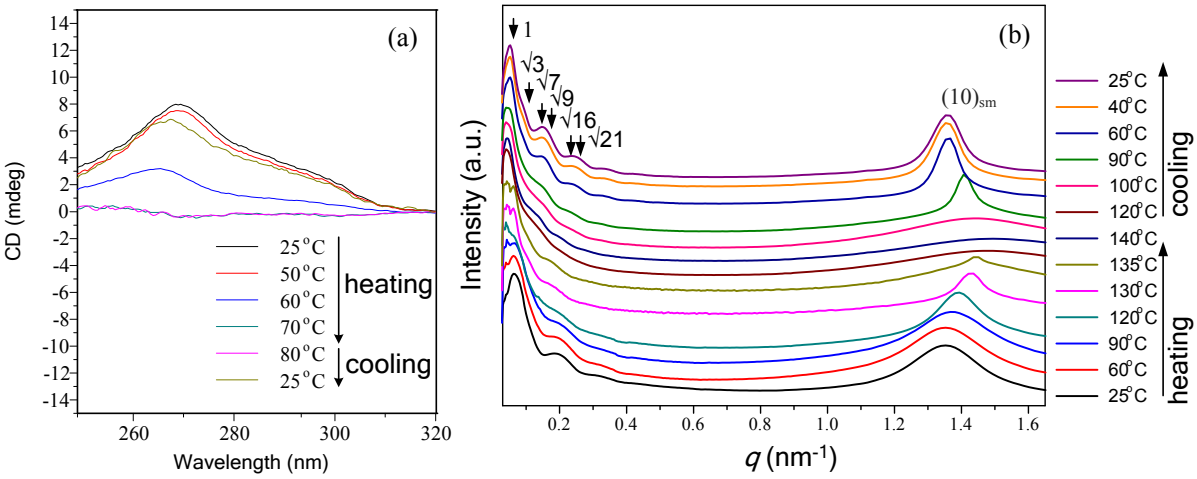

Figure S8. (a) temperature-dependent CD spectra of $P4VP_{8.8K}(\mathbf{aD})_{0.5}$ (0.05 mass % in trichloromethane). (b) temperature-dependent SAXS profiles of PS_{151K}-*b*-$P4VP_{163K}(\mathbf{aD})_{0.5}$.

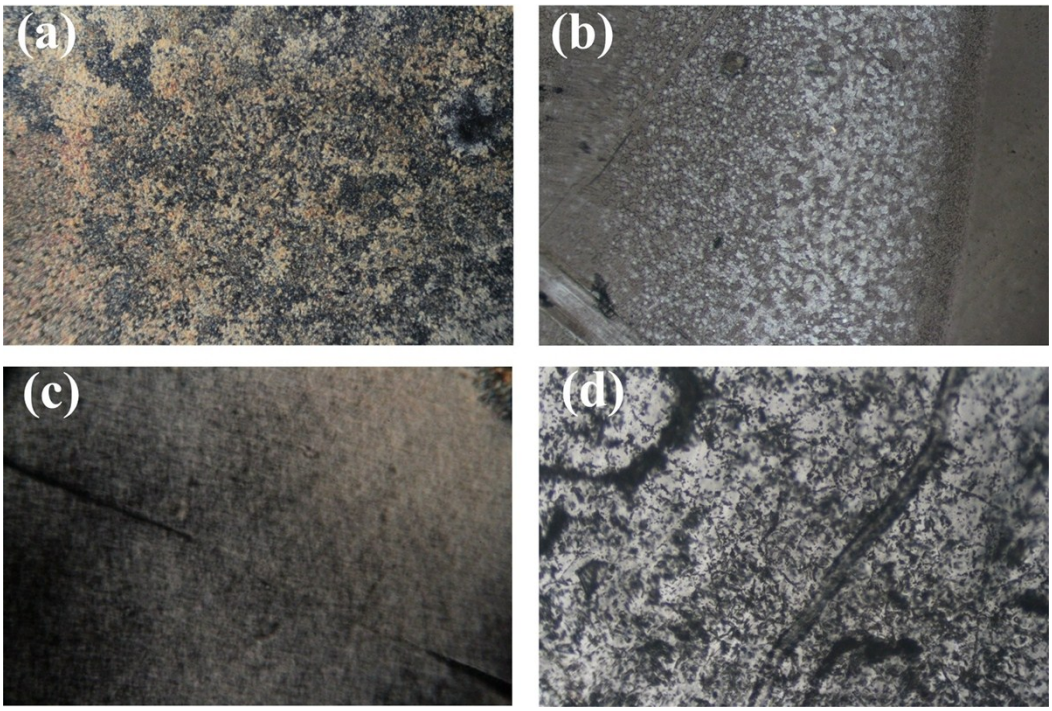

Figure S9. POM images (a) PS_{151K}-*b*-$P4VP_{163K}(\mathbf{aD})_{0.5}$, (b) PS_{75K}-*b*-$P2VP_{113K}(\mathbf{aD})_{0.3}$, (c) PS_{248K}-*b*-$P2VP_{195K}(\mathbf{sD})_{0.75}$, (d) PS_{151K}-*b*-$P4VP_{163K}(\mathbf{sD})_{0.5}$.

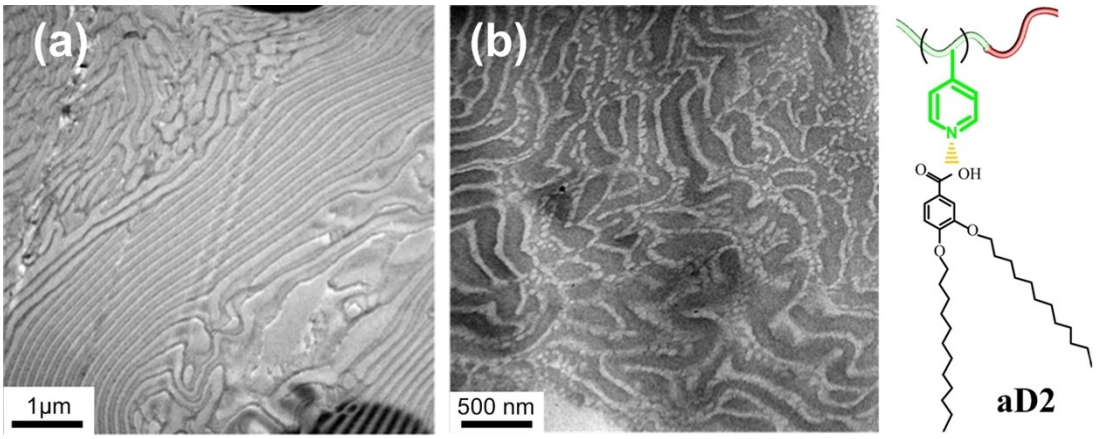

Figure S10. TEM images of PS_{151K}-*b*-$P4VP_{163K}$(**aD2**)$_x$ with x=0.3 (a) and 0.5 (b). The inset is a schematic chemical structure of PS_{151K}-*b*-$P4VP_{163K}$(**aD2**)$_x$.

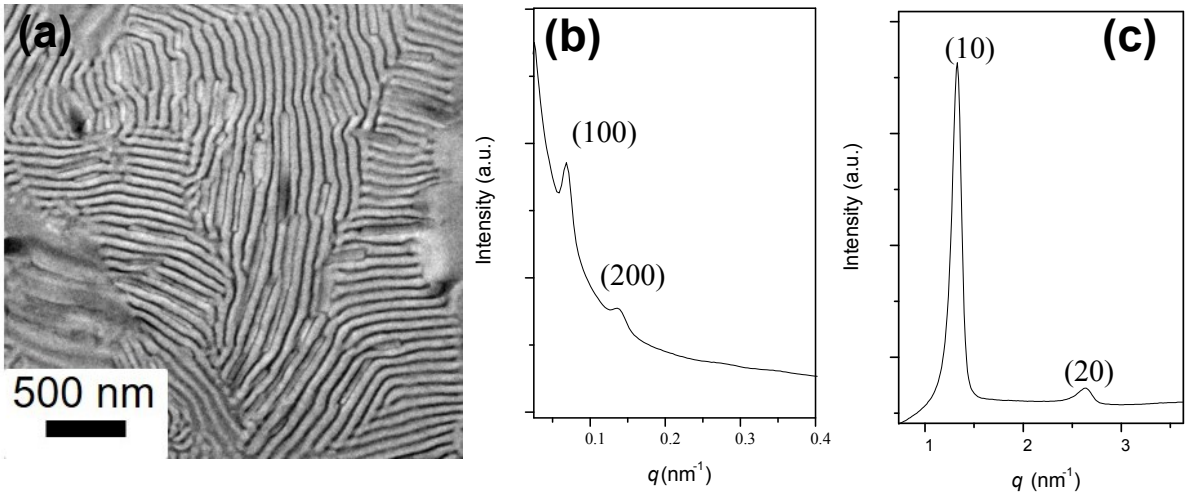

Figure S11. (a) TEM image, (b) SAXS and (c) WAXD profiles of PS_{240K}-*b*-$P4VP_{20K}$(**aD**)$_{0.6}$.

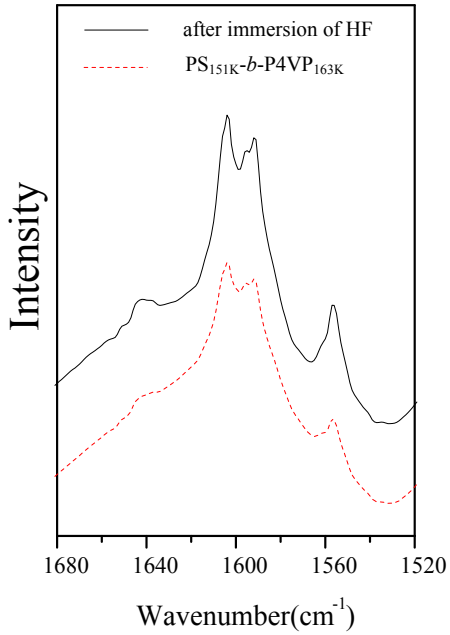

Figure S12. FTIR spectrum (solid line) of PS_{151K}-*b*-$P4VP_{163K}$(**aD**)$_{0.5}$ after immersion in hydrogen fluoride to remove **aD** and for protonation of P4VP. FTIR spectrum (broken line) of neat PS_{151K}-*b*-$P4VP_{163K}$ shown as control.

3,4-Bis(4-octyloxybenzyloxy)benzoic acid (aD). ^{1}H NMR (500 MHz, $CDCl_3$): δ = 7.69–7.68 (m, 2H), 7.37–7.32 (m, 4H), 6.96 (d, J = 8.5 Hz, 1H), 5.15 (s, 2H), 5.11 (s, 2H), 3.96 (t, J = 6.5 Hz, 4H), 1.80–1.77 (m, 4H), 1.46–1.44 (m, 4H), 1.34–1.29 (m, 16H), 0.89 (t, J = 6.5 Hz, 6H).

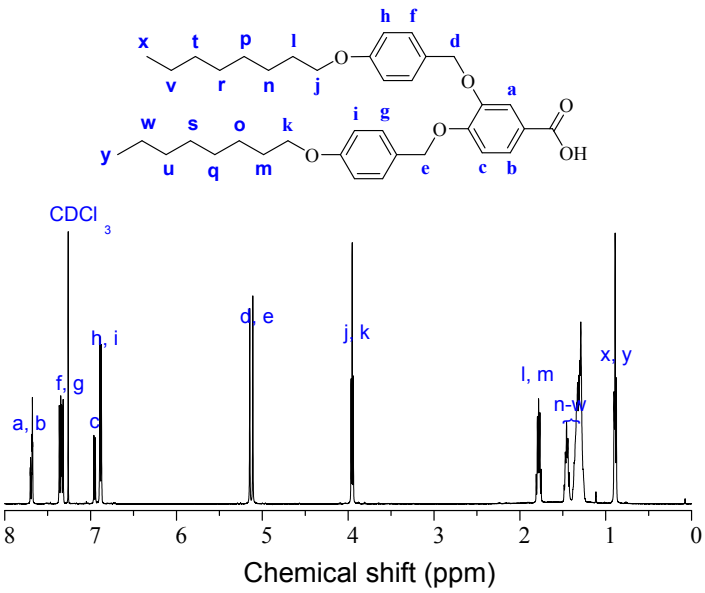

Figure S13. ^{1}H NMR spectrum of **aD** in $CDCl_3$.

3,5-Bis(4-octyloxybenzyloxy)benzoic acid (sD). ^{1}H NMR (500 MHz, $CDCl_3$): δ = 7.35–7.33 (m, 6H), 6.91 (d, J = 8.5 Hz, 4H), 6.83 (s, 1H), 5.00 (s, 4H), 3.97 (t, J = 6.5 Hz, 4H), 1.80–1.77 (m, 4H), 1.46–1.29 (m, 20H), 0.89 (t, J = 6.5 Hz, 6H).

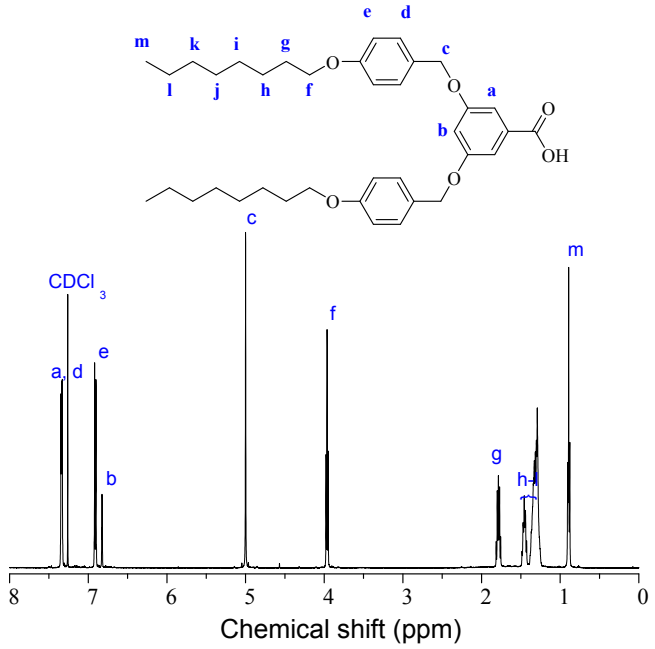

Figure S14. ^{1}H NMR spectrum of **sD** in $CDCl_3$.

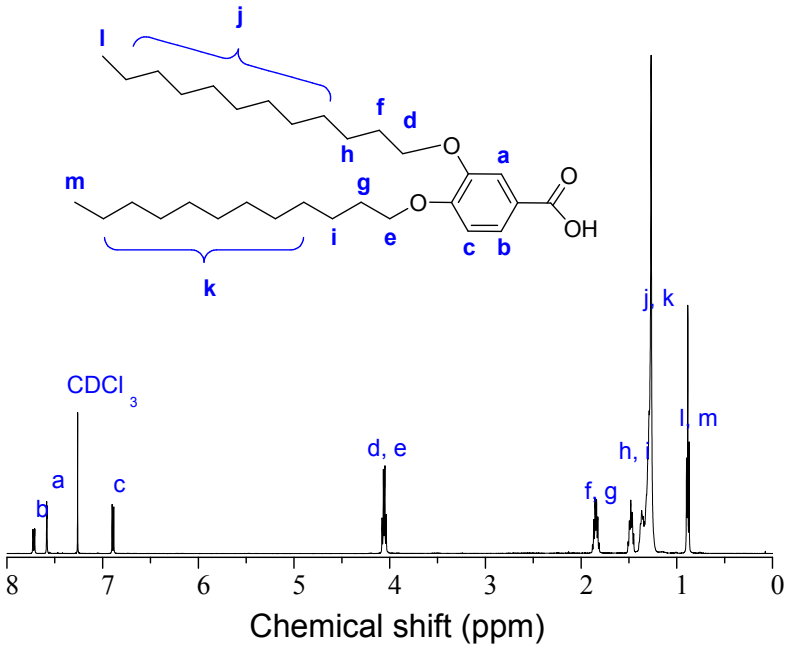

Figure S15. ^{1}H NMR spectrum of **aD2** in $CDCl_3$.

Scheme S1. Synthetic Routes and Chemical Structures of **aD** and **sD**.[a]

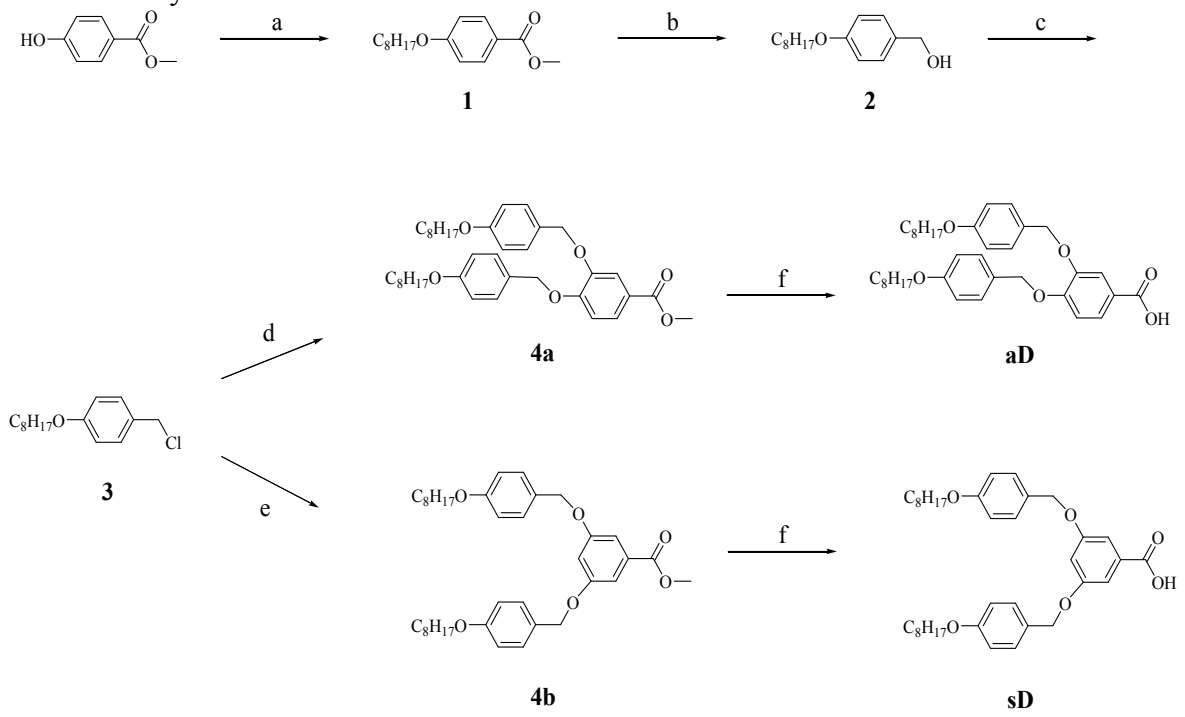

[a]Reagents and conditions: (a) 1-bromooctane, K_2CO_3, KI, acetone, reflux, 48 h; (b) $LiAlH_4$, THF, 50 °C, overnight; (c) $SOCl_2$, DMF (a drop, catalyst), dichloromethane, 25 °C, 5 h; (d) methyl 3,4-dihydroxybenzoate, K_2CO_3, [18]crown-6, acetone, reflux, 48 h; (e) methyl 3,5-dihydroxybenzoate, K_2CO_3, [18]crown-6, acetone, reflux, 48 h; (f) 2.5 M $KOH_{(aq)}$, THF/EtOH (7:3, v/v), reflux, overnight, then acidified with 6 M $HCl_{(aq)}$.

Scheme S2. Synthetic Routes and Chemical Structures of **aD2**[b]

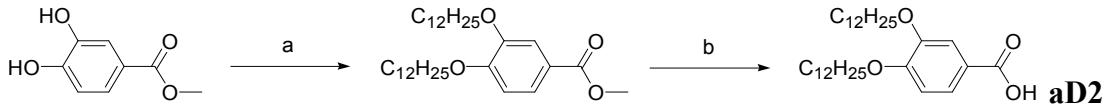

[b]Reagents and conditions: (a) 1-bromododecane, K_2CO_3, KI, acetone, reflux, 48 h; (b) 2.5 M KOH(aq, THF/EtOH (7:3, v/v), reflux, overnight, then acidified with 6 M HCl(aq).

Table S1. Characteristics of pyridine-based BCP and homopolymers

Sample	PS (g mol^{-1})	P4VP or P2VP (g mol^{-1})	M_w/M_n	ϕ_{PS}
PS_{151k}-*b*-$P4VP_{163k}$	151,000	163,000	1.2	0.5
PS_{248k}-*b*-$P2VP_{195k}$	248,000	195,000	1.08	0.58
PS_{75K}-*b*-$P2VP_{113K}$	75,000	113,000	1.2	0.41
PS_{240K}-*b*-$P4VP_{20K}$	240,000	20,000	1.1	0.93
$P4VP_{8.8K}$	–	8,800	1.1	–
$P2VP_{26K}$	–	26,000	1.05	–

Table S2. Lattice parameters of DJBCPs

Sample	ϕ_{PS}	d_{100}	a	d_{10}
			(nm)	
PS_{151k}-*b*-$P4VP_{163k}$(**aD**)$_{0.5}$	0.23	120	130	4.6
PS_{151k}-*b*-$P4VP_{163k}$(**sD**)$_{0.5}$	0.23	106	122	3.9
PS_{75k}-*b*-$P2VP_{113k}$(**aD**)$_{0.3}$	0.23	76	88	3.7
PS_{248k}-*b*-$P2VP_{195k}$(**sD**)$_{0.75}$	0.23	136	157	3.0